Radiation Protection Dosimetry (2013), Vol. 155, No. 3, pp. 329–334 doi:10.1093/rpd/nct011
Advance Access publication 7 February 2013

IMPACT OF THE X-RAY SYSTEM SETTING ON PATIENT DOSE AND IMAGE QUALITY; A CASE STUDY WITH TWO INTERVENTIONAL CARDIOLOGY SYSTEMS

J. Vassileva[1,*], E. Vano[2], C. Ubeda[3], M. Rehani[4] and R. Zotova[1]
[1]National Centre of Radiobiology and Radiation Protection, Sofia, Bulgaria
[2]Radiology Department, Complutense University, Madrid, Spain
[3]Clinical Science Department, Health Sciences Faculty and CIHDE, Tarapaca University, Arica, Chile
[4]International Atomic Energy Agency, Vienna, Austria

*Corresponding author: j.n.vassileva@gmail.com

Received September 18 2012, revised November 18 2012, accepted January 14 2013

This study investigates the influence of the initial X-ray system setting on patient doses and image quality in interventional cardiology procedures. Two dedicated interventional cardiology systems were studied: a system with image intensifier (II) and a flat detector (FD) system. Entrance surface air kerma (ESAK) rates in fluoroscopy and ESAK per frame in the acquisition mode were measured on the surface of a PMMA phantom for the field of views (FOV) of 23 and 17 cm (II system) and 25 and 20 cm (FD system). Signal-to-noise ratio (SNR) and contrast-to-noise ratio (CNR) were estimated using DICOM images obtained during the measurements. System performances were compared using a figure of merit combining SNR and ESAK. The influence of system setting on patient doses was investigated analysing the information for air kerma area product (KAP) and cumulative dose (CD) at the patient entrance reference point, for a sample of coronary angiography examinations. ESAK rates in fluoroscopy modes were a factor of 2 higher in the FD system for the similar FOVs, resulting in a factor of 1.9 higher median values of KAP and CD for patients with FD system than for the II system. SNR and CNR for the FD system were better than the equivalent FOVs with II. The resulting FOM was better for the FD system in both FOVs. Potential for optimisation was suggested by adjusting system settings.

INTRODUCTION

Interventional cardiology procedures are rapidly increasing during last years. A number of international and national studies demonstrated large variation in patient doses in similar examinations, which can be attributed to differences in the complexity of procedures but also to different settings of the X-ray systems[1–5]. Current fluoroscopy systems fall into two distinct categories: image intensifier (II) and flat detector (FD). An II is a large vacuum tube that captures the pattern of X-ray radiation transmitted through the patient and converts it into a light image of sufficient brightness to be seen on the television camera. This system has been utilised for radiology imaging since the 1960s. Soon after their development, II was coupled with television systems to enable viewing of fluoroscopic images; the modern II systems are equipped with a charge-coupled device. FD systems represent the most modern solid-state detector technology used as the image receptor, based on large arrays of amorphous silicon photodiodes and thin film transistors in combination with CsI (Tl) scintillators, which has the potential to improve image quality with less radiation dose than II[6, 7].

Interventional X-ray systems are equipped with different operational modes like 'fluoroscopy mode', 'digital subtraction angiography (DSA) acquisition mode', and 'cine acquisition mode'. Manufacturers use different automatic exposure control curves and beam shaping filters to maintain the required image quality[8]. It is also possible to configure the initial system parameters (e.g., pulse rate, pulse width, X-ray tube current, X-ray tube voltage, filtration and focal-spot size) with various optional adjustments by the installation service engineers. Clinical protocols are often locally adapted depending on the clinical task and local preferences by changing the system parameters used in fluoroscopy and image acquisition modes. Thus, the same given model of imaging system installed at different locations could have vast differences in image quality and patient doses.

An important step when starting patient dose surveys is to characterise the system performance by measuring the important operating parameters of X-ray systems. The protocol for commissioning or characterisation of an X-ray fluoroscopy system was well standardised within the European SENTINEL Concerted Action and used for interventional radiology and cardiology[9–11]. This protocol is being applied by several hospitals in Europe during the acceptance and status tests of the interventional fluoroscopy systems. There are several studies in the literature which investigate the performance in terms

of dose and image quality between different angiographic systems with these protocols[6, 12, 13]; however, only a few have used an ionisation chamber as a radiation detector and profit the image of the chamber to evaluate image quality parameters, when the test object was not available or the access to the X-ray systems is restricted due to the high clinical workload[14].

The same approach was also adopted in the protocol for commissioning of modern fluoroscopy systems in Bulgaria, including that for interventional radiology and cardiology. It contains X-ray system characterisation by measurements of dose and image quality with a standard polymethyl methacrylate (PMMA) phantom of different thicknesses for different operational modes[15]. This study investigates the influence of the initial X-ray system setting on patient doses and image quality in interventional cardiology procedures. Results from routine quality control performed on two particular II and FD systems were used to study the systems settings and to suggest optimisation actions. Results of patient doses over a sample of clinical procedures are also included to support the convenience of optimisation actions.

MATERIALS AND METHODS

Angiography equipment

Two X-ray systems dedicated to interventional cardiology were included in the investigation. System A was a Siemens Axiom Artis FC (Siemens Healthcare, Germany), equipped with an II and three fields of views (FOVs) with diameters of 23, 17 and 13 cm, three fluoroscopy modes, named 'fluoro-' (low), 'fluoro' (normal) and 'fluoro+' (high) and digital cine acquisition modes with 15 and 30 frames per second (fr s^{-1}). Additional copper (Cu) filters of thickness 0.2–0.9 mm are automatically inserted into the beam to reduce skin dose. System B was a Philips Allura Xper FD10 (Philips Healthcare, The Netherlands), equipped with a flat panel imaging receptor, named hereafter FD, with three FOVs: 25, 20 and 15 cm (diagonal), three fluoroscopy modes (low, normal and high), acquisition cine modes with 3.75, 7.5, 15 and 30 fr s^{-1} and with 0.9 mmCu in the low fluoroscopy mode, 0.4 mmCu in the medium mode and 0.1 mmCu for the high fluoroscopy mode (+1 mm Al in all the cases).

Measurements of entrance surface air kerma

Entrance surface air kerma (ESAK) rate in the fluoroscopy mode and ESAK per frame in the acquisition cine mode were measured with a shadow-free ionisation chamber type TW 34069 and dosemeter UNIDOS E (PTW Freiburg, Germany). Standard size patient was simulated with a PMMA phantom of 20 cm thickness and cross-sectional dimensions of 25 cm × 25 cm. The ionisation chamber was positioned in contact with the PMMA phantom closely between the patient couch and the phantom in order to measure ESAK including the backscatter radiation[16]. The ESAK rate in fluoroscopy and ESAK per frame in the acquisition cine mode were measured for the most often used FOVs of 23 and 17 cm (system A) and 25 and 20 cm (system B). Measurements of ESAK rate for both systems were performed at the acquisition cine mode with 15 fr s^{-1} that is the most often used rate in clinical procedures. For systems A and B, the distance from the isocentre to the floor was 107 and 106 cm and the distance from the focus to the isocentre was 66 and 65 cm, respectively (Figure 1). Filtration and details of radiographic techniques for the different modes were not registered (except for cine acquisition which was included as part of the DICOM header information), but they were the standard for Siemens and Philips systems.

Image quality estimation

All the series of images acquired during the dose measurements (fluoroscopy and cine acquisition) were archived in DICOM format and later analysed numerically to estimate signal-to-noise ratio (SNR) and contrast-to-noise ratio (CNR) values. The method described elsewhere was used for SNR estimation using the plastic wall of the ionisation chamber as a low contrast object[14]. The advantage of this simple method is the simultaneous measurement of dose and image quality estimation. Results using dedicated test objects are more reliable, but sometimes, the availability of the catheterisation laboratories for quality control tests is scarce and measurements need to be made in only a few hours. Regions of interest (ROI) of similar sizes (650–750 pixels) were selected in the wall of the ionisation chamber (ROI 1) and in the background outside the

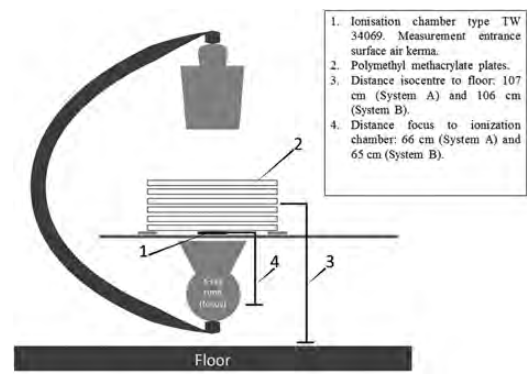

Figure 1. Geometry of measurement of ESAK using PMMA phantom and ionisation chamber.

chamber wall (ROI 2) (Figure 2). The SNR is defined as[6, 14, 17, 18]:

$$\mathrm{SNR} = \frac{\mathrm{BG} - \mathrm{ROI}}{\sqrt{(\mathrm{STD}^2_{\mathrm{ROI}} + \mathrm{STD}^2_{\mathrm{BG}})/2}}, \quad (1)$$

where BG is the mean value of the pixel contained in the ROI 2 outside the chamber wall, and ROI the mean value of the pixel contained in the ROI 1 in the chamber wall; STD the corresponding standard deviation for the pixel content in the selected ROIs, inside and outside the chamber wall.

Three measurements were made for ROIs in the wall and outside the wall. SNR values reported for each image are mean values from the three corresponding calculations.

Similar approach was used to calculate the CNR, defined as:

$$\mathrm{CNR} = \frac{\mathrm{BG} - \mathrm{ROI}}{\sqrt{\mathrm{BG}}}, \quad (2)$$

where BG and ROI are the same as used for SNR calculation[17].

The overall system performance was estimated with a figure of merit (FOM) combining SNR and ESAK as follows [6, 17–19]:

$$\mathrm{FOM} = \frac{\mathrm{SNR}^2}{\mathrm{ESAK}}. \quad (3)$$

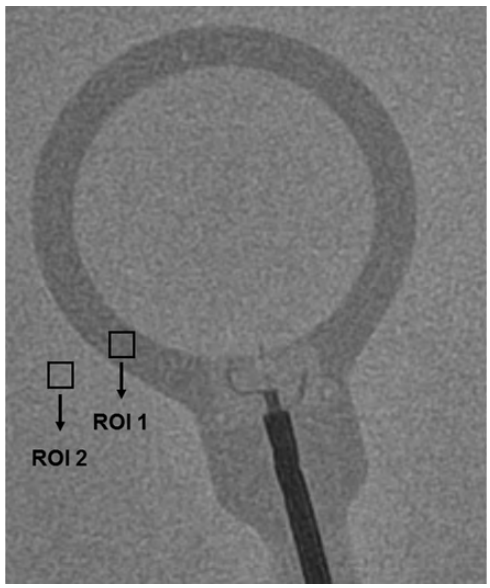

Figure 2. Example of image obtained with the FD system B (FOV 25 cm).

In order to investigate the influence of the X-ray system setting on patient doses, dose information was extracted from patient dose reports produced by both X-ray systems, for a sample of coronary angiography (CA) examinations of a number of procedures performed in adult patients. Samples consisted of 54 patients for system A and 58 patients for system B. The following information was extracted from patient files: age and weight of the patient, total fluoroscopy time, number of acquired cine series and acquisition cine images, as well as the total air kerma area product (KAP) and the cumulative dose (CD) at the patient entrance reference point[16, 20]. The later is located along the central ray of the X-ray beam at a distance of 15 cm from the isocentre in the direction of the focal spot and is representative for the patient skin at the entrance site of the X-ray beam[20]. All collected dose values expressed in KAP and CD for both systems were corrected by the particular measured calibration factor that takes into account the attenuation of the table and the mattress. This approach is recommended by the International Code of Practice for Dosimetry in Diagnostic Radiology and was used in the survey performed during the European Research Program SENTINEL[21, 22]. For each sample, statistical analysis was performed by calculating minimum, maximum, mean and median values.

RESULTS

Results for the ESAK rate for the 20 cm PMMA phantom in different fluoroscopy modes for most often used FOVs with systems A and system B are presented in Figure 3.

Table 1 shows the numerical values of ESAK per frame, SNR and CNR in the acquisition mode (15 fr s^{-1}) for the most often used FOVs with both systems: FOV 23 and 17 cm in system A and FOV 25 and 20 cm in system B. Results for the calculated FOM are presented in the last column of Table 1.

Patient doses for a sample of CA procedures for both systems are presented in Table 2. The mean, median, minimum and maximum values of the following parameters are shown: age and weight of the patient, total fluoroscopy time, number of acquired cine series and acquisition cine images, as well as total KAP and CD.

DISCUSSION

For system A (with II), the increase in the ESAK rate in the normal fluoroscopy mode is higher by a factor of 2.3 when switching from FOV 23 cm to FOV 17 cm (Figure 3). Figure 3 shows for system B (with FD) that this increment was equivalent to a factor of 1.3 when changing from FOV 25 to FOV

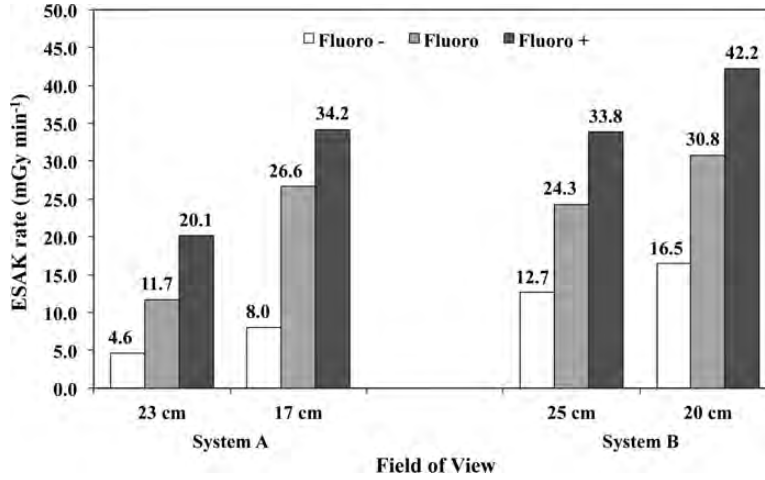

Figure 3. ESAK rate at the 20 cm PMMA phantom in PA projection for both systems in all fluoroscopy modes.

Table 1. Exposure parameters [tube voltage (kV), tube current (mA) and filtration (mmCu), ESAK per frame, SNR, CNR and FOM] for different fields of view in the cine acquisition mode (15 fr s^{-1}) with system A and system B.

FOV (cm)	Exposure parameters, kV, mA, mmCu	ESAK/frame, μGy fr^{-1}	SNR	CNR	FOM $\times$ 100, μGy^{-1}
System A					
23	65, 799, 0.3	72.6	1.97	0.41	5.33
17	68, 759, 0.1	166.0	2.71	0.52	4.45
System B					
25	68, 466, [a]	154.3	3.09	1.18	6.23
20	69, 577, [a]	203.6	3.03	1.20	4.52

[a]Unavailable information.

17. The same factors of increment between both FOV, 2.3 for system A and 1.3 for system B were found for the cine mode, as seen from data in Table 1. The found increase in the ESAK values for the II system can be mainly attributed to the geometrical minification factor that is 1.83 when switching from 23 to 17 cm field size. The observed variations in the increase factor between different modes (from 1.7 to 2.3) can be explained by differences in the automatic gain control reference adjustment, as well as differences in scatter conditions, depending on the beam quality (tube voltage and filtration) used in different modes.

Results in Figure 3 show an abnormal increase in the ESAK rate in system A setting, when switching between low and normal fluoroscopy modes: by a factor of 2.5 for the FOV 23 cm, and by a factor of 3.3 for the FOV 17 cm. The similar increase in the ESAK rate for system B is by a factor of 1.9 for the FOV 25 cm and by a factor of 1.4 for the FOV 20 cm.

The comparison of the absolute values of ESAK per frame in the cine mode for the similar FOVs of both systems (Table 1) demonstrates that system B performs with a factor of 2.1 higher ESAK than system A.

When comparing the results achieved for both systems in terms of the ESAK rate for low fluoroscopy modes and ESAK per frame for the cine mode, with the reference levels proposed by Padovani *et al.*[3] for cardiology equipment, the values were lower for the system A in both modes. Values for system B were equal (12.7 mGy min^{-1}) and higher (154.3 μGy per frame), respectively. Other authors [6, 23] also have reported ESAK values for fluoroscopy modes and the cine acquisition mode in this range of values. One of the papers[6]

Table 2. Patient doses during CA examinations for 54 patients with system A and 58 patients with system B.

Parameter	System A			System B		
	Mean	Median	Min–Max	Mean	Median	Min–Max
Age, y	62	61	37–82	59	57	46–75
Weight, kg	76	73	58–128	73	74	55–98
Fluoroscopy time, min	2.6	1.8	0.7–10.4	2.9	2.5	0.8–11.5
Number of series	10	10	6–16	9	10	6–15
Number of images	571	560	287–918	602	575	322–936
KAP total, Gy cm^2	16.0	15.0	3.8–36.0	28.1	29.9	7.3–54.6
CD total, mGy	267.3	246.4	70.8–599.0	420.5	453.4	111.3–675.1

presents the evaluation of a Siemens Axiom Artis FC system configured with an II and later upgraded to an FD. The ESAK values reported in this article were lower for the II and higher for the FD system. Regarding the second one[23], the reported values were 13 mGy min^{-1} for the low fluoroscopy mode, 34 mGy min^{-1} for the normal fluoroscopy mode and 38 mGy min^{-1} for the high fluoroscopy mode, for a Philips Integris 3000 system. During the cine mode, the reached dose rate was 163 μGy per frame. Ubeda *et al.*[18] reported for a national survey in Chile, the differences in dose settings and image quality among 10 X-ray systems used in adult interventional cardiology procedures and found a range from 7.9 to 39.7 mGy min^{-1} for the low fluoroscopy mode, 17.5 to 115.1 mGy min^{-1} for the normal fluoroscopy mode, 27.7 to 121.7 mGy min^{-1} for the high fluoroscopy mode and 123.7 to 338.8 μGy per frame for the cine mode.

The influence of system setting on patient doses is seen from Table 2. For CA, in both systems are used similar clinical protocols, similar projections and the same frame rate for the cine mode of 15 fr s^{-1}. The fluoroscopy time for system A was between 0.7 and 10.4 min and for system B was between 0.8 and 11.5 min; the mean number of acquisition cine frames was 571 for system A and 602 for system B. The total median values of KAP and CD for the examination with system B was around a factor of 1.9 higher than for system A. This can be explained by the higher ESAK values in fluoroscopy and cine modes in system B.

Test objects are usually used to evaluate image quality during acceptance or commissioning tests and later for constancy checks. More simple practical approach was applied in this study by analysing images of the flat ionisation chamber used for dose measurements. In this case, results of SNR and CNR of system B were better than with system A for the equivalent FOVs (Table 1). Because the quality of clinical images is considered satisfactory for cardiologists using system A, the possibility to evaluate a low-dose protocol (using low-dose per pulse in fluoroscopy and cine or increasing the added copper filtration) should be considered for system B.

As shown in Table 1, for the FOV of 23–25 cm, SNR was higher for system B (3.09 for system B and 1.97 for system A), assuring better image quality with more capability to visualise low contrast objects. This is in correspondence to the higher dose per frame for system B, 154 at 72.6 μGy fr^{-1} for system A. For the FOV 17–20 cm, SNR was similar between both systems 2.71 and 3.03, respectively, corresponding to the almost similar dose per frame values, 166 and 203.6, respectively. The increase in SNR and ESAK with decrease in FOV for system A is abnormally high, indicating at the non-optimised setting of this system.

The CNR is not changing significantly with the FOV, but this parameter resulted much better for system B and cardiologists should probably realise this improvement in image quality with the FD system. The FD system uses higher tube voltage (68–69 kV in acquisition) and less filtration (0.1 mmCu in acquisition) to improve the contrast, but this results in higher ESAK values.

The FOM, defined to have a global numerical indication combining ESAK and image quality, resulted 2–17% better for system B in both FOVs (Table 1).

CONCLUSIONS

This case study with only two digital fluoroscopy systems was not aimed at setting objective criteria for optimisation in terms of SNR, CNR or FM. However, it indicates that dose measurements performed as a part of routine quality control of digital angiography systems may be used to obtain objective image quality indexes and to compare between different X-ray systems settings. This information can be used to optimise the initial system setting and to detect failures or mistakes. SNR/CNR measured together with dose parameters for different fluoroscopy and cine modes can help clinicians selecting

the appropriate imaging mode for different clinical tasks.

This approach applied to the investigated II angiography systems found abnormal increase in SNR and ESAK with decrease in FOV, indicating at the non-optimised setting of this system. Better image quality parameters but higher ESAK values in fluoroscopy and cine modes were found for the FD system, resulting in higher median values of KAP and CD for the patient examinations. Usually, higher ESAK values involve better image quality and the balance benefit–risk needs to be considered by the industry during the different initial system setting of the X-rays systems and the user should be informed on the adopted criteria. Possibility for dose reduction with the FD system using low-dose per pulse in fluoroscopy and cine or increasing added copper filtration was suggested to be investigated. Using a standard FOM for comparison, the FD system presented better balance between image quality and dose.

REFERENCES

1. Neofotistou, V., Vano, E., Padovani, R., Kotre, J., Dowling, A., Toivonen, M., Kottou, S., Tsapaki, V., Willis, S., Bernardi, G. *et al*. *Preliminary reference levels in interventional cardiology*. Eur. Radiol. **13**(10), 2259–2263 (2003).
2. Hart, D., Hillier, M. and Wall, B. *Doses to Patients from Radiographic and Fluoroscopic X-ray Imaging Procedures in the UK—2005 Review*. HPA-RPD-029. Health Protection Agency (2007).
3. Padovani, R., Vano, E., Trianni, A., Bokou, C., Bosmans, H., Bor, D., Jankowski, J., Torbica, P., Kepler, K., Dowling, A. *et al*. *Reference levels at European level for cardiac interventional procedures*. Radiat. Prot. Dosim. **129**(1–3), 104–107 (2008).
4. Balter, S., Miller, D. L., Vano, E., Ortiz Lopez, P., Bernardi, G., Cotelo, E., Faulkner, K., Nowotny, R., Padovani, R. and Ramirez, A. *A pilot study exploring the possibility of establishing guidance levels in x-ray directed interventional procedures*. Med. Phys. **35**(2), 673–680 (2008).
5. Miller, D. L., Kwon, D. and Bonavia, G. H. *Reference levels for patient radiation doses in interventional radiology: proposed initial values for U.S. practice*. Radiology **253**(3), 753–764 (2009).
6. Vano, E., Geiger, B., Schreiner, A., Back, C. and Beissel, J. *Dynamic flat panel detector versus image intensifier in cardiac imaging: dose and image quality*. Phys. Med. Biol. **7**, 5731–5742 (2005).
7. Davies, A., Cowen, A., Kengyelics, S., Moore, J. and Sivananthan, M. *Do flat detector cardiac x-ray systems convey advantages over image-intensifier based systems? Study comparing x-ray dose and image quality*. Eur. Radiol. **17**, 1787–1794 (2007).
8. Lin, P. J. *The operation logic of automatic dose control of fluoroscopy system in conjunction with spectral shaping filters*. Med. Phys. **34**, 3169–3172 (2007).
9. Zoetelief, J., Schultz, F. W., Kottou, S., Gray, L., O'Connor, U., Salat, D., Kepler, K., Kaplanis, P., Jankowski, J., Schreiner, A. *et al*. *Quality control measurements for fluoroscopy systems in eight countries participating in the SENTINEL EU coordination action*. Radiat. Prot. Dosim. **129**(1–3), 237–243 (2008).
10. Tsapaki, V., Padovani, R., Vano, E., Schreiner, A., Molfetas, M., Neofotistou, V. and Kottou, S. *Commissioning and constancy protocols for digital angiographic units*. Radiat. Prot. Dosim. **129**(1–3), 258–260 (2008).
11. Padovani, R., Trianni, A., Bokou, C., Bosmans, H., Jankowski, J., Kottou, S., Kepler, K., Malone, J., Tsapaki, V., Salat, D. *et al*. *Survey on performance assessment of cardiac angiography systems*. Radiat. Prot. Dosim. **129**(1–3), 108–111 (2008).
12. Tsapaki, V., Kottou, S., Kollaros, N., Dafnomili, P., Koutelou, M., Vano, E. and Neofotistou, V. *Comparison of a conventional and a flat-panel digital system in interventional cardiology procedures*. Br. J. Radiol. **77**, 562–567 (2004).
13. Vano, E., Ubeda, C., Martinez, L. C., Leyton, F. and Miranda, P. *Paediatric interventional cardiology: flat detector versus image intensifier using a test object*. Phys. Med. Biol. **55**(23), 7287–7297 (2010).
14. Vano, E., Ubeda, C., Fernandez, J. M., Sanchez, R. M. and Prieto, C. *Dose assessment during the commissioning of flat detector imaging systems for cardiology*. Radiat. Prot. Dosim. **136**(1), 30–37 (2009).
15. Dimov, A. and Vassileva, J. *Assessment of performance of a new digital image intensifier fluoroscopy system*. Radiat. Prot. Dosim. **129**(1–3), 123–126 (2008).
16. International Commission on Radiation Units and Measurements (ICRU). *Patient dosimetry for X rays used in medical imaging*. ICRU report 74. ICRU (2005).
17. Vano, E., Ubeda, C., Leyton, F. and Miranda, P. *Radiation dose and image quality for paediatric interventional cardiology*. Phys. Med. Biol. **53**, 4049–4062 (2008).
18. Ubeda, C., Vano, E., Miranda, P., Leyton, F., Valenzuela, E. and Oyarzun, C. *Radiation dose and image quality for adult interventional cardiology in Chile. A national survey*. Radiat. Prot. Dosim. **147**(1–2), 90–93 (2011).
19. Samei, E., Dobbins, J., Lo, J. and Tornai, M. *A framework for optimising the radiographic technique in digital x-ray imaging*. Radiat. Prot. Dosim. **114**, 220–229 (2005).
20. International Electrotechnical Commission. *Medical electrical equipment—Part 2-43: Particular requirements for the basic safety and essential performance of X-ray equipment for interventional procedures*. Edition 2.0 2010-03. Report IEC 60601–2–43. IEC (2010).
21. International Atomic Energy Agency. Dosimetry in Diagnostic Radiology. An International Code of Practice. TRS 457. Vienna (2007).
22. Jankowski, J., Domienik, J., Papierz, S., Padovani, R., Vano, E. and Faulkner, K. *An international calibration of kerma-area product meters for patient dose optimisation study*. Radiat. Prot. Dosim. **129**(1–3), 328–332 (2008).
23. Vano, E., Gonzalez, L., Fernandez, J. M., Prieto, C. and Guibelalde, E. *Influence of patient thickness and operation modes on occupational and patient radiation doses in interventional cardiology*. Radiat. Prot. Dosim. **111**, 297–304 (2006).